The Arctic picoeukaryote *Micromonas pusilla* benefits synergistically from warming and ocean acidification

Clara J. M. Hoppe[1,2]*, Clara M. Flintrop[1,3] and Björn Rost[1]

[1] Marine Biogeosciences, Alfred Wegener Institute – Helmholtz Centre for Polar and Marine Research, 27570 Bremerhaven, Germany

[2] Norwegian Polar Institute, 9296 Tromsø, Norway

[3] MARUM, 28359 Bremen, Germany

*Correspondence to: Clara J. M. Hoppe (Clara.Hoppe@awi.de)

Abstract

In the Arctic Ocean, climate change effects such as warming and ocean acidification (OA) are manifesting faster than in other regions. Yet, we are lacking a mechanistic understanding of the interactive effects of these drivers on Arctic primary producers. In the current study, one of the most abundant species of the Arctic Ocean, the prasinophyte *Micromonas pusilla*, was exposed to a range of different pCO_2 levels at two temperatures representing realistic current and future scenarios for nutrient-replete conditions. We observed that warming and OA synergistically increased growth rates at intermediate to high pCO_2 levels. Furthermore, elevated temperatures shifted the pCO_2-optimum of biomass production to higher levels. Based on changes in cellular composition and photophysiology, we hypothesise that the observed synergies can be explained by beneficial effects of warming on carbon fixation in combination with facilitated carbon acquisition under OA. Our findings help to understand the higher abundances of picoeukaryotes such as *M. pusilla* under OA, as has been observed in many mesocosm studies.

1 Introduction

With the progress in using molecular tools to describe marine biodiversity in the past decades, the scientific community has become increasingly aware of the underestimated importance of picoeukaryotes, for both primary and export production of the world's oceans (Richardson and Jackson, 2007; Worden and Not, 2008). Larger phytoplankton such as diatoms are efficient vectors for carbon export due to aggregate formation and ingestion by large zooplankton leading to the production of fast-settling faecal pellets (Sherr et al., 2003). In contrast, picoeukaryotes are mainly grazed by smaller heterotrophic protists such as ciliates, which have a low carbon retention, excrete relatively more dissolved material, and thus fuel recycled production (Sherr and Sherr, 2002). Hence, changes in the relative abundance of pico- and nanoeukaryotes can have large implications for food webs and biogeochemistry (Worden et al., 2015).

Picoeukaryotes tend to dominate low nutrient environments, which is often attributed to their high surface:volume ratios and mixotrophic capacities (Raven, 1998; McKie-Krisberg and Sanders, 2014). The low nutrient concentrations in the Arctic surface ocean, for example, cause picoeukaryotes to be particularly successful in this region. In fact, the globally occurring prasinophyte *Micromonas pusilla* is considered the most abundant species in the Arctic ocean (Šlapeta et al., 2006; Lovejoy et al., 2007; Marquardt et al., 2016). In this environment, strong stratification causes low nutrient concentrations throughout the summer and autumn months (Tremblay et al., 2015), and the occurrence of the polar night requires organisms to either form resting stages or to have heterotrophic capacities (Tremblay et al., 2009; Lovejoy, 2014; Berge et al., 2015; Vader et al., 2015).

Climate change effects manifest faster in the Arctic than anywhere else on the planet (Stocker, 2014). In this region, for example, temperatures are rising more than twice as fast as at the rest of the globe (Miller et al., 2010). The concurrent rapid reduction in ice cover allows for more light penetration and longer growing seasons, while increased stratification due to ice melt and warming constrain nutrient supply to surface waters, both of which will change the dynamics of primary production (Arrigo et al., 2008; Wassmann and Reigstad, 2011). Ocean acidification (OA) is also especially pronounced in the Arctic Ocean, because low temperatures and alkalinity make the system sensitive to anthropogenic CO_2 loading (AMAP, 2013; Qi et al., 2017). Picoeukaryotes such as *M. pusilla* may benefit from these changes and are considered potential winners of climate change. In the Canadian Arctic, for example, picoeukaryote abundances are increasing as surface waters get warmer, fresher and more oligotrophic (Li et al., 2009). Regarding OA effects, the majority of studies on natural phytoplankton assemblages

62 have shown picoeukaryotes, particularly *M. pusilla*, to increase in relative abundance with

63 increasing pCO_2 levels (Engel et al., 2008; Meakin and Wyman, 2011; Newbold et al., 2012;

64 Brussaard et al., 2013; Hussherr et al. 2017; Schulz et al., 2017). Despite the evident sensitivity

65 of *M. pusilla* to changes in pCO_2 levels, a detailed assessment of the OA effects, their

66 interaction with warming as well as the underlying mechanisms in this important species is still

67 missing.

68 Like all photosynthetic organisms, cells of *M. pusilla* need to maintain a balance

69 between energy sources (i.e. light harvesting by the photosynthetic apparatus) and sinks (most

70 importantly carbon fixation in the Calvin cycle) to prevent harmful levels of excitation pressure

71 on the photosynthetic electron transport chain (Behrenfeld et al., 2008). Light harvesting and

72 electron transport in the photosystems are largely independent of changes in temperature and

73 pCO_2 (Mock and Hoch, 2005; Hoppe et al., 2015), but the impact of these drivers on energy

74 sinks can potentially affect the energy balance of the cell: The beneficial effects of elevated

75 pCO_2 observed in phytoplankton are thought to be caused by increased diffusive CO_2 supply,

76 reduced CO_2 leakage, or by lowered costs to operate their CO_2 concentrating mechanisms (Rost

77 et al., 2008; Bach et al., 2013). Elevated temperatures, on the other hand, can change enzyme

78 kinetics including those involved in the Calvin cycle, thus leading to a larger sink of excitation

79 energy (Maxwell et al., 1994; Toseland et al., 2013). Hence, both ocean warming and

80 acidification potentially increase the efficiency of photosynthesis and biomass production, at

81 least up to the organisms' respective optimum levels. Above these levels, temperatures and

82 proton concentrations start to disrupt enzymatic processes, increase the investment into pH

83 homeostasis, and impair the delicate regulation of cellular processes (Levitt, 1980; Taylor et

84 al., 2001; Flynn et al., 2012). Thus, the complex balance between beneficial and detrimental

85 effects will determine whether the combination of warming and OA will synergistically

86 promote or deteriorate phytoplankton growth and biomass build-up.

87 In the current study, we aim to investigate the responses of an Arctic *M. pusilla* strain

88 to warming and OA. To this end, *M. pusilla* was grown at four pCO_2 levels ranging from

89 preindustrial to future scenarios (180-1400 µatm) under 2°C and 6°C, which represent the

90 magnitude of the projected future temperature increase in this region (Collins et al., 2013), but

91 also the current spring and summer temperatures in the environment where the strain was

92 isolated (Hegseth et al., in press).

2 Material & Methods

2.1 Culture conditions

Monoclonal cultures of the picoeukaryote *Micromonas pusilla* (Butcher) I. Manton & M. Parke (isolated in 2014 by K. Wolf in Kongsfjorden, Svalbard, 79°N; local temperature range -1.5 to 8°C) taxonomic identification confirmed by rDNA sequencing of SSU, LSU and ITS sequences) were grown in 1-L glass bottles in semi-continuous dilute-batch cultures (max 129,000 cells mL^{-1}; diluted every 3-4 days) under constant irradiances of 150 ± 26 µmol photons m^{-2} s^{-1}. Media consisted of 0.2 µm sterile-filtered Arctic seawater with a salinity of 32.7 enriched with macronutrients, trace metals and vitamins according to F/2$_R$ medium (Guillard and Ryther, 1962). Light intensities were provided by daylight lamps (Philips Master TL-D 18W; emission peaks at wavelength of 440, 560 and 635 nm), adjusted by neutral density screens and monitored using a LI-1400 data logger (Li-Cor) equipped with a 4π-sensor (Walz). Cells were growing at four different CO_2 partial pressures (pCO_2; 180, 380, 1000, and 1400 µatm) and two temperatures (2.2 ± 0.3°C and 6.3 ± 0.2°C). Cultures were acclimated to these conditions for at least 7 generations prior to sampling.

Different pCO_2 conditions were achieved by aeration of the incubation bottles with air of the respective pCO_2 levels delivered through sterile 0.2-µm air-filters (Midisart 2000, Sartorius stedim) for 24 h prior to inoculation. Gas mixtures were generated using a gas flow controller (CGM 2000 MCZ Umwelttechnik), in which CO_2-free air (<1 ppmv CO_2; Dominick Hunter) was mixed with pure CO_2 (Air Liquide Deutschland). The pCO_2 levels in the gas mixtures were regularly monitored with a non-dispersive infrared analyzer system (LI6252, LI-COR Biosciences), calibrated with CO_2-free air and purchased gas mixtures of 150 ±10 and 1000 ±20 ppmv CO_2 (Air Liquide Deutschland).

2.2 Carbonate chemistry

Samples for total alkalinity (A$_T$) were filtered through 0.7-µm glass fibre filters (GF/F, Whatman) and stored in borosilicate bottles at 3°C. A$_T$ was estimated from duplicate potentiometric titration (Brewer et al., 1986) using a TitroLine alpha plus (Schott Instruments). A$_T$ values were corrected for systematic errors based on measurements of certified reference materials (CRMs provided by Prof. A. Dickson, Scripps, USA; batch #111; reproducibility ±5 µmol kg^{-1}). Total dissolved inorganic carbon (C$_T$) samples were filtered through 0.2-µm cellulose-acetate filters (Sartorius stedim) and stored in gas-tight borosilicate bottles at 3°C. C$_T$ was measured colorimetrically in triplicates with a QuAAtro autoanalyzer (Seal; Stoll et al.

127 2001). The analyser was calibrated with $NaHCO_3$ solutions (with a salinity of 35, achieved by

128 addition of NaCl) to achieve concentrations ranging from 1800 to 2300 µmol C_T kg^{-1}. CRMs

129 were used for corrections of errors in instrument performance such as baseline drifts

130 (reproducibility ±8 µmol kg^{-1}). Seawater pH_{total} was measured potentiometrically with a two-

131 point calibrated glass reference electrode (IOline, Schott Instruments). An internal TRIS-based

132 reference standard (Dickson et al., 2007) was used to correct for variability on electrode

133 performance (reproducibility ±0.015 pH units). Following recommendations by Hoppe et al.

134 (2012), seawater carbonate chemistry including pCO_2 was calculated from A_T and pH using

135 CO_2SYS (Pierrot et al., 2006). The dissociation constants of carbonic acid of Mehrbach et al.

136 (1973), as refitted by Dickson and Millero (1987), were used for calculations. Dissociation

137 constants for $KHSO_4$ were taken from Dickson (1990).

138

2.3 Growth, elemental composition and production rates

140 Samples for cell counts were fixed with glutaraldehyde (0.5% final concentration). After gentle

141 mixing, samples were stored at room temperature in the dark for 15 min, and subsequently

142 frozen in liquid nitrogen and stored at -80°C. Prior to analysis, samples were thawed on ice and

143 mixed thoroughly. After addition of 10 µL SybrGreen working solution (dissolved in DMSO)

144 and 10 µL YG beads working solution (1µm-Flouresbrite calibration beads grade YG,

145 Polyscience), samples were counted on an Accuri C6 flow cytometer (BD Biosciences)

146 equipped with a blue solid-state laser (488 nm excitation wavelength) run on medium fluidics

147 settings (35 µL min^{-1}; 16 µm core size) with a limit of 50,000 events or 250 µL. Analysis was

148 performed based on red (FL3 channel, >670 nm) and green (FL1 channel, 533 ± 30 nm)

149 fluorescence, as well as sideward and forward light scattering. Specific growth rates constants

150 (µ) were determined from exponential fits of cell counts over 4 consecutive days.

151 Particulate organic carbon (POC) and nitrogen (PON) were measured after filtration

152 onto precombusted (15h, 500 °C) GF/F filters (Whatman) and stored at -20 °C. and dried for

153 at least 12 h at 60 °C prior to sample preparation. Analysis was performed using a CHNS-O

154 elemental analyser (Euro EA 3000, HEKAtech). Contents of POC and PON were corrected for

155 blank measurements and normalised to filtered volume and cell densities to yield cellular

156 quotas. Production rates of POC were calculated by multiplying the cellular quota with the

157 division rate constant k of the respective incubation. Samples for determination of chlorophyll

158 a (Chl a) were filtered onto GF/F filters (Whatman), immediately placed into liquid nitrogen

159 and stored at -80°C until analysis. Chl a was subsequently extracted in 8 mL 90% acetone at

160   4°C over night. Chl *a* concentrations were determined on a fluorometer (TD-700, Turner

161   Designs), using an acidification step (1M HCl) to determine phaeopigments (Knap et al., 1996).

162

163   **2.4 Variable Chl *a* fluorescence**

164   Photophysiological characteristics, based on photosystem II (PSII) variable Chl *a* fluorescence,

165   were measured using a fast repetition rate fluorometer (FRRf; FastOcean PTX, Chelsea

166   Technologies) in combination with a FastAct Laboratory system (Chelsea Technologies). The

167   excitation wavelength of the fluorometer's light-emitting diodes (LEDs) was 450 nm, and the

168   applied light intensity was 21587 µmol photons m^{-2} s^{-1}. The FRRf was used in single turnover

169   mode, with a saturation phase comprising 100 flashlets on a 2 µs pitch and a relaxation phase

170   comprising 40 flashlets on a 50 µs pitch. Measurements from all replicates (n=3) were

171   conducted in a temperature-controlled chamber (±0.2°C) at the respective treatment

172   temperature.

173   After subtraction of a blank value, the minimum (F_0 and F_0' for light-and dark-

174   acclimated measurements, respectively) and maximum Chl *a* fluorescence (F_m, and F_m' for

175   light-and dark-acclimated measurements, respectively) were estimated from iterative

176   algorithms for induction (Kolber et al., 1998) and relaxation phase (Oxborough, 2012) after 15

177   min of dark acclimation, which was sufficient to achieve a dark-acclimated state (data not

178   shown). All fluorescence parameters were calculated by standard equations (Genty et al., 1989;

179   Maxwell and Johnson, 2000). Maximum quantum yields of PSII (apparent PSII photochemical

180   quantum efficiency; F_v/F_m) were calculated as

181        $F_v/F_m = (F_m-F_0)/F_m$ (1)

182   Fluorescence based photosynthesis-irradiance curves (PI) were conducted at six irradiances (I)

183   between 33 and 672 µmol photons m^{-2} s^{-1}, with an acclimation time of 10 min per light step.

184   Electron transfer rate through PSII (ETR [mol e^- (mol RCII)$^{-1}$ s^{-1}]) for each light step was

185   calculated as:

186        $ETR = ((F_m'-F_0')/F_m') * I$ (2)

187   Following the suggestion by Silsbe and Kromkamp (2012), the light-use efficiency (α [mol e^-

188   m^2 (mol RCII)$^{-1}$ (mol photons)$^{-1}$]) and the maximum electron transfer rates per RCII (ETR_{max}

189   [mol e^- (mol RCII)$^{-1}$ s^{-1}]) were estimated by fitting the data to the model by (Webb et al., 1974):

190        $ETR = ETR_{max} * [1-e^{(-(\alpha*I)/ETR_{max})}]$ (3)

191   The light saturation index (E_k [µmol photons m^{-2} s^{-1}]) was then calculated as ETR_{max}/α.

192   Maximum non-photochemical quenching of Chl *a* fluorescence (NPQ) at irradiances of 672

193 µmol photons m^{-2} s^{-1} (i.e. the highest irradiance step of the PI curve) were calculated using the

194 normalized Stern-Volmer coefficient, also termed NSV, as described in McKew et al. (2013):

195 $\quad (F_q'/F_v')-1 = F_0'/F_v'$ (4)

196 where F_q' is the differences between measured and maximal fluorescence (Suggett et al., 2010).

197 F_0' was measured after each light step (with a duration of 90 s).

198

199 **2.5 Statistics**

200 All data is given as the mean of three biological replicates with ± one standard deviation. To

201 test for significant differences between the treatments, two-way analyses of variance (ANOVA)

202 with additional normality (Kolmogorov-Smirnov) and Post Hoc (Holm-Sidak) tests were

203 performed. The significance level was set to 0.05. Statistical analyses were performed with the

204 program SigmaPlot (SysStat Software Inc, Version 12.5).

205

206 **3 Results**

207

208 **3.1 Carbonate Chemistry**

209 Regular dilution of cultures with pre-aerated seawater medium kept carbonate chemistry stable

210 over the course of the experiment. More specifically, in each bottle the drift in A_T and C_T

211 compared to initial values was $\leq 3\%$ and $\leq 4\%$, respectively (data not shown). Final carbonate

212 chemistry in the 2°C treatments yielded pCO_2 levels of 197 ± 3, 323 ± 12, 959 ± 22 and 1380

213 ± 53 µatm (Table 1). In the 6°C treatments, pCO_2 levels were 198 ± 6, 394 ± 10, 1036 ± 31 and

214 1449 ± 18 µatm. Please note that the same pCO_2 level translates into differing dissolved CO_2

215 concentrations at different temperatures due to the temperature dependency of the carbonate

216 system. Specifically, the treatment pCO_2 values translated into up to 13% lower dissolved CO_2

217 concentrations in the 6°C compared to the 2°C treatment (Table 1; cf. Figure SI1).

218 Concurrently, the pCO_2 levels at 2°C corresponded to pH_{total} values of 8.30 ± 0.01, 8.11 ± 0.01,

219 7.68 ± 0.01 and 7.52 ± 0.02, respectively. In the 6°C treatment, pH_{total} values of the four pCO_2

220 treatments were 8.30 ± 0.01, 8.04 ± 0.01, 7.65 ± 0.01 and 7.52 ± 0.01, respectively.

221

222 **3.2 Growth and biomass build-up**

223 Growth rates constants of exponentially growing *M. pusilla* cultures were significantly affected

224 by the applied treatments (Figure 1, Table 2, SI1). Depending on the pCO_2 level, temperature

225 increased growth by 20 to 60% with an average of 0.80 d^{-1} under low and 1.10 d^{-1} under high

226 temperature conditions (two-way ANOVA, F = 328, p <0.001). Overall, there was also a

227 positive pCO_2 effect on growth (two-way ANOVA, F = 9, p = 0.001), even though no linear

228 trends with either pCO_2 or $[CO_2]$ were observed (Figure 1, SI1). The observed pCO_2 responses

229 also differed between temperature levels, indicating a significant interaction between both

230 drivers (two-way ANOVA, F = 12, p <0.001): Under low temperature, growth increased

231 significantly from 180 to 380 µatm pCO_2 (post-hoc, t = 3.1, p = 0.04), while there was a

232 declining, yet insignificant trend in growth with further increases in pCO_2. Under high

233 temperature, growth was significantly higher under 1000 compared to lower (180 µatm; post-

234 hoc, t = 5.6, p <0.001) and higher pCO_2 levels (1400 µatm; post-hoc, t = 5.9, p <0.001). Thus,

235 warming shifted the optimum range for growth to higher pCO_2 levels (Figure 1A).

236 This trend was also observed in terms of POC production rates (Figure 1B, Table 2),

237 with significant effects of temperature (Table SI1; two-way ANOVA, F = 356, p <0.001), pCO_2

238 (two-way ANOVA, F = 7, p = 0.003), and their interaction (two-way ANOVA, F = 29, p

239 <0.001). At low temperatures, higher production rates were observed at 180 and 380 µatm

compared to those at 1000 and 1400 µatm pCO_2 (post-hoc tests, t = 3.5, p = 0.016 and t = 3.0, p = 0.046, respectively). At high temperatures, POC production rates were significantly higher at 1000 µatm than at all other pCO_2 levels (post-hoc tests, e.g. t = 9.1, p <0.001 for 380 vs. 1000 µatm and t = 7.4, p <0.001 for 1000 vs. 1400 µatm), again indicating an upward shift in the pCO_2 optimum with warming.

3.3 Cellular composition

Overall, POC quota (Figure 2 a, Table 2, Table SI1) were significantly higher under elevated compared to low temperature (two-way ANOVA, F = 24, p <0.001), but no overarching trend with pCO_2 was observed. Under low temperature, cells had significantly higher POC quota at low pCO_2 levels (180 and 380 µatm) compared to high pCO_2 levels (1000 and 1400 µatm; all four post-hoc tests significant, e.g. 380 vs 1000µatm: t = 2.8, p = 0.033). This trend reversed under high temperature, where POC quota were highest under 1000 and 1400 µatm (post-hoc test, t = 3.5, p = 0.024). Thus, temperature and pCO_2 levels exhibited a significant interactive effect on POC quota (two-way ANOVA, F = 10, p <0.001).

Similar trends were observed in terms of cellular PON quota (Figure 2 b, Table 2, Table SI1), where temperature (two-way ANOVA, F = 5, p = 0.045) and its interaction with pCO_2 (two-way ANOVA, F = 10, p <0.001) significantly affected the results. Here, opposing pCO_2 effects under different temperatures were more subtle, with PON quota under low temperatures only being significantly decreased between 380 and 1400 µatm (post-hoc test, t = 3.3, p = 0.027), while under high temperature PON quota significantly increased from 180 and 380 to 1000 µatm pCO_2 (post-hoc tests, t = 3.7, p = 0.012 and t = 2.8, p = 0.028, respectively).

Regarding cellular Chl *a* quota, there were no significant effects of temperature or pCO_2 alone (Figure 2 c, Table 2, Table SI1), but a significant interaction between the two drivers (two-way ANOVA, F = 18, p <0.001): Under low temperature, Chl *a* quota decreased from low (180 µatm) to high pCO_2 levels (1000 and 1400 µatm; post-hoc tests, t = 5.0, p <0.001 and t = 3.9, p = 0.006, respectively). Under high temperature, the opposite trend was observed, where Chl *a* quota increased from low (180 and 380 µatm) to high pCO_2 levels (1000 and 1400 µatm; all four post-hoc tests significant, e.g. 380 vs 1000µatm: t = 3.0, p = 0.027).

Molar C:N ratios of the biomass (Table 2, Table SI1) increased with temperature (two-way ANOVA, F = 14, p = 0.002), yet this overall difference was mainly driven by results at low pCO_2 levels (180 and 380 µatm; post-hoc tests, t = 2.7, p = 0.017 and t = 3.5, p = 0.003, respectively). By itself, pCO_2 did not significantly affect C:N ratios.

The ratios of C:Chl *a* (Figure 2 d, Table 2, Table SI1) were elevated under high

274   compared to low temperature conditions (two-way ANOVA, F = 14, p = 0.002), an effect that

275   was most pronounced at pCO_2 levels of 180 µatm (post-hoc test, t = 5.5, p <0.001). While there

276   was no effect of pCO_2 on C:Chl a at low temperature, C:Chl a decreased with increasing pCO_2

277   at high temperature (two-way ANOVA, interaction term, F = 6, p = 0.007; 180 vs. 1400 µatm

278   at 6°C post-hoc test, t = 3.9, p = 0.008).

279

280   **3.4 Chl a fluorescence-based photophysiology**

281   The effects of the applied treatments on photophysiology were studied by means of FRRf,

282   which investigates photochemistry at photosystem II (PSII). No effects of the applied

283   treatments were observed in most parameters investigated (Table 3, SI1). This was true for the

284   dark-acclimated quantum yield efficiency of PSII (F_v/F_m), which was similar in all treatments

285   with values of 0.45 ±0.06, as well as for absorption cross section of PSII light harvesting (σ_{PSII}).

286   Furthermore, the fitted parameters of FRRf-based PI curves (α, ETR_{max} and E_K) were

287   independent of the experimental treatments (Table 3, SI1). In contrast, the rate constant of the

288   reopening of PSII reaction centres (τ_{ES}; Table 3, SI1) was slightly yet significantly smaller

289   under high temperatures (two-way ANOVA, F = 6, p = 0.029), even though this overall

290   response also depended on the applied pCO_2 levels (two-way ANOVA, interaction term, F = 4,

291   p = 0.033).

292   Maximum non-photochemical quenching (NPQ_{max}; Table 3, SI1) increased

293   significantly with pCO_2 (Table SI1; two-way ANOVA, F = 0, p = 0.002) while temperature had

294   no effect. Post-hoc tests revealed that this response was mainly driven by high NPQ_{max} values

295   at 1000 µatm, which were significantly higher than in any other pCO_2 treatment (e.g. t = 4.1, p

296   = 0.006 for 380 vs. 1000 µatm and t = 3.1, p = 0.030 for 1000 vs. 1400 µatm).

4 Discussion

4.1 *Micromonas pusilla* benefits from warming

We observed a strong stimulation of growth rates and biomass build-up with increasing temperature (Figure 1, Table 2). Even though the isolate stems from 1.8°C water temperature, the beneficial effects of warming from 2°C to 6°C are not surprising: *M. pusilla* is known to dominate Arctic phytoplankton assemblages in the summer and autumn situations (Lovejoy et al., 2007; Marquardt et al., 2016) when surface temperatures of 6°C or more can be reached (Hegseth et al., in press). Our results are also in line with mesocosm experiments that indicate stimulatory effects of warming on picoplankton abundances (Daufresne et al., 2009; Sommer et al., 2015) as well as with the temperature optimum of 6-8°C observed for another Arctic strain of *M. pusilla* (Lovejoy et al., 2007).

Below the temperature optimum of a cell, warming causes an acceleration of the entire metabolism, as enzymatic reactions run faster under these conditions (Eppley, 1972; Brown et al., 2004). In this study, warming caused higher growth rates, POC quotas and biomass production (Figure 2, Tables 2, SI1), indicating that particularly the fixation and storage of carbon was facilitated by increasing temperature. Electron transport processes, on the other hand, were largely independent of temperature (Tables 3, SI1). Thus, temperature affected the balance between electron transport ('light reaction') and carbon fixation in the Calvin cycle ('dark reactions'). Especially under relatively low temperatures, as investigated here, warming can decrease the excitation pressure on the electron transport chain of the photosystems by increasing the temperature-limited turnover rates of enzyme reaction such as RuBisCO (Mock and Hoch, 2005). Thus, cells grown under low temperature need to invest relatively more energy into biosynthesis than into photochemistry compared to cells grown under high temperature (Toseland et al., 2013). While it has been shown that Antarctic diatoms can compensate for slow RuBisCO kinetics by increasing the expression of this enzyme (Young et al., 2014), it is unknown whether such acclimation responses also occur in prasinophytes. Regarding the C:Chl *a* ratio, this can be taken as an in indicator on how much resources the cell retains as carbon biomass (e.g. structural and storage compounds) relative to how much is invested into its light harvesting capacities (Halsey and Jones, 2015). In this study, the strong temperature-dependent increase in C:Chl *a* (Figure 2, Table SI1) under potentially limiting pCO_2 levels of 180 µatm suggests that under warming, the balance between light harvesting and carbon fixation was indeed more beneficial for biomass build-up. Furthermore, elevated temperature significantly decreased τ_{ES} (Table 3, SI1), which can serves as a proxy of the rate

331 at which down-stream processes can remove electrons from PSII (Kolber et al., 1998). Thus,
332 our results indicate that the drainage of electrons into carbon fixation was faster under warmer
333 conditions, explaining the higher growth and biomass production under these conditions.
334

4.2 Warming shifts CO₂ optima towards higher pCO₂ levels

336 Under 6°C and pCO₂ levels expected to be reached by the end of this century, OA had a
337 significantly positive effect on growth and biomass build-up (Figure 1). This finding is in line
338 with previous studies, which have shown that picoeukaryotes can benefit strongly from OA in
339 both laboratory and mesocosm studies (Meakin and Wyman, 2011; Newbold et al., 2012;
340 Schaum et al., 2012; Brussaard et al., 2013; Maat et al., 2014; Schulz et al., 2017). Such positive
341 response to OA could indicate that picoeukaryotes such as *M. pusilla* are mainly dependent on
342 diffusive CO₂ supply and thus directly benefit from higher CO₂ concentrations (Brussaard et
343 al., 2013; Schulz et al., 2013; Schulz et al., 2017). While this could be related to the large surface
344 to volume ratio of small cells, opposite trends within the group of diatoms (i.e. higher sensitivity
345 of larger compared to smaller diatoms; Wu et al.; 2014; Sett et al. 2018) suggest more complex
346 underlying mechanisms at play.

347 Despite this overall effect, growth rates of *M. pusilla* tended to follow a non-linear
348 response curve over the tested range of glacial to elevated future pCO₂ levels (i.e. 180 to 1400
349 µatm), i.e. growth increased with increasing pCO₂ from low to intermediate, but decreased
350 again under the highest pCO₂ levels (Figure 1). Such an optimum behaviour can be expected
351 for most environmental drivers (Harley et al., 2017) and has previously been observed in
352 response to OA (Sett et al., 2014; Wolf et al., 2018). The response patterns in these studies were
353 attributed to a combination of beneficial effects of rising pCO₂ under potentially carbon-
354 limiting conditions for photosynthesis, and negative effects of declining pH on cellular
355 homeostasis and enzyme performance, which manifest mainly at high pCO₂ (Bach et al., 2013).
356 This non-linearity in the observed pCO₂ effects emphasises the importance of experiments with
357 more than two pCO₂ levels in order to properly describe OA-response patterns of organisms.

358 On a more general level, apparent discrepancies between OA studies can be attributed
359 to actual differences in the environmental settings and their interactive effects with pCO₂
360 (Riebesell and Gattuso, 2015). When comparing the two most commonly applied pCO₂ levels,
361 i.e. the present-day and the anticipated end-of-century situation, the effects of OA on most of
362 the investigated physiological parameters are reversed under 6°C compared to 2°C (Figure 3).
363 This illustrates how difficult it is to infer responses to OA from experiments applying only one
364 set of environmental conditions. It is also noteworthy that the combination of OA and warming

365 led to more densely packed cells (no change in cell size based on flow cytometric

366 measurements; data not shown) with similar stoichiometry compared to the control treatment

367 (Table 2). This indicates that cells managed to cope well with the experienced future conditions.

368 Furthermore, warming altered the OA-dependent change in most of the investigated parameters

369 in a direction that indicates higher fitness compared to low temperatures (e.g. higher growth

370 rates and higher elemental quota; Figure 3). Thus, the increase in growth under future compared

371 to ambient conditions was larger than what would be expected by the respective responses to

372 warming and OA in isolation, indicating synergistic beneficial effects of both drivers.

373

374 **4.3 Potential mechanism underlying the interaction between warming and OA**

375 The observed synergistic effects could be explained by their specific impacts on carbon

376 acquisition and fixation. As outlined in the introduction, light and dark reaction of

377 photosynthesis need to be balanced to achieve high biomass production while avoiding

378 photodamage (Behrenfeld et al., 2008). According to our data, this balance is shifted towards

379 higher biomass production rates under warming and OA.

380   At higher temperatures, seawater CO_2 concentrations were lower than under colder

381 conditions (Table 1; Zeebe and Wolf-Gladrow, 2001). At the same time, warming from 2°C to

382 6°C caused up to 60% higher growth and 110% higher biomass build-up rates (Figure 1, Table

383 2). Furthermore, the decrease in τ_{ES} indicates a faster transfer of photochemical energy into

384 downstream processes such as RuBisCO activity (Table 3). Increased carbon demand in concert

385 with lower carbon supply at higher temperatures thus increases the risk of CO_2 shortage in the

386 cell, which in turn causes OA to have larger effects than at colder temperatures. Moreover,

387 warming changes the kinetics of carbon fixation, with RuBisCO increasing its maximum

388 turnover rates but decreasing its affinity for CO_2 (Young et al., 2014). At higher temperature,

389 cells thus have the potential for higher carboxylation rates provided sufficient CO_2 is available

390 (Kranz et al., 2015). Under elevated pCO_2 levels, diffusive CO_2 supply increases and/or costs

391 for active carbon acquisition decrease. Consequently, the positive effect of increasing

392 temperature on the carbon fixation rate can develop its full potential under OA.

393   In conclusion, elevated catabolic activity under warmer conditions can explain the

394 observed upward shift in the CO_2-optimum of growth with increasing temperature (Figure 1),

395 as the corresponding higher carbon demand causes CO_2 fixation to saturate under higher pCO_2

396 levels. In combination with a faster and more efficient machinery for pH homeostasis at

397 elevated temperatures (Morgan-Kiss et al., 2006), this could explain why declining growth rates

398   were only observed at relatively higher pCO_2 levels compared to those under low temperature

399   conditions (Figure 2).

4.4 Implications for the current and future Arctic pelagic ecosystem

Picoeukaryotes such as *M. pusilla* are considered to be potential winners of climate change: They are not only thriving in warmer, more stratified environments, which are predicted to further expand in the future, but also seem to benefit from OA (Li et al., 2009; Schulz et al., 2017). Our results for *M. pusilla* confirm beneficial effects of warming and OA on growth and biomass production under nutrient-replete conditions (Figure 1, Table 2). Hence, in warmer spring conditions of the future, this species may experience growth stimulation under OA, potentially increasing its importance early in the growing season. Currently, *M. pusilla* already dominates Arctic phytoplankton assemblages in the nutrient-limited summer and autumn situations, which were not investigated in this study. Regarding the importance of nutrient availability, laboratory experiments found beneficial OA effects on *M. pusilla* primary production to persist also under P limitation (Maat et al., 2014), while in a mesocosm community, OA-dependent increases in *M. pusilla* abundances disappeared when the system ran into P and N co-limitation (Engel et al., 2008). Thus, it remains to be seen how the combined effects of warming and OA manifest under low nutrient conditions as well as how the responses may depend on sources and types of nutrients (e.g. mixing-delivered nitrate vs. regenerated ammonium).

A species' success in the environment does not only depend on individual performance, but also on how it compares to that of competing species. When we compare our results with the responses of the Arctic diatom *Thalassiosira hyalina*, isolated from the same location and exposed to the same experimental conditions (Wolf et al., 2018), the diatom had higher growth rates than the picoeukaryote under most treatment conditions, as can be expected for nutrient-replete conditions (Sarthou et al., 2005). The relative increase in growth rates from ambient (2 or 3°C and 380 µatm pCO_2) to future conditions (6°C and 1000 µatm pCO_2) was, however, much higher for *M. pusilla* than for *T. hyalina*. The fact that our experiments were conducted under nutrient-replete conditions, which typically favour diatoms over picoeukaryotes, may indicate an even stronger increase in fitness (Collins et al., 2014) and could mean that *M. pusilla* gains another competitive advantage over phytoplankton like diatoms in the future, in addition to those resulting from changes in stratification (Li et al., 2009). Thus, our findings suggest higher picoplankton contribution to future Arctic phytoplankton assemblages under non-limiting conditions, e.g. early in the growing season when picoeukaryotes can already contribute quite substantially to the phytoplankton standing stocks (Marquardt et al, 2017, Paulsen et al. 2015). How such competition between diatoms and picoeukaryotes would

manifest under nutrient-depleted conditions that strongly favour *M. pusilla* is currently unknown.

Even though picoeukaryotes seem to contribute more to the downward export of organic matter than previously assumed (Waite et al., 2000; Richardson and Jackson, 2007), in comparison to e.g. diatoms, they are less efficient vectors for carbon export to depth and have a lower energy transfer along trophic levels (Sherr et al., 2003). Consequently, Arctic food webs dominated by picoeukaryotes would look very different from those fuelled by diatom production (Sherr et al., 2003; Paulsen et al., 2015). Due to its motility and capability to grow mixotrophically, *M. pusilla* is characterized by an exceptionally high cellular C:N ratio compared to other Arctic phytoplankton (Table 2; Halsey et al., 2014; McKie-Krisberg and Sanders, 2014). An increased importance of this species would thus not only affect the food web due to its small size and concurrent grazer preferences, but also in terms of food quality (van de Waal and Boersma, 2012). The expected higher growth rates and thus abundances of this species may thus strengthen the Arctic microbial food web. Together with a concurrent weakening of the classical diatom-fuelled food web, this could have severe implications for the flow of energy and nutrients through future marine Arctic ecosystems (Post, 2016).

4.5 Conclusions

This study is the first to show synergistic effects of warming and OA on *M. pusilla*, one of the most abundant species of the worlds' oceans. Individually, both warming and OA cause more efficient biomass build-up under nutrient-replete conditions. Beneficial effects manifest, however, even more strongly in combination, when facilitated carbon acquisition (e.g. due to higher diffusive CO_2 supply) co-occurs with higher fixation rates (e.g. due to higher turnover-rates of RuBisCO). Our results provide an explanation for the observations of previous mesocosm studies, which indicated beneficial effects of OA and warming on *M. pusilla* and other picoeukaryotes. Characterising the responses of this Arctic key species to warming and OA will help to develop mechanistic phytoplankton functional types and more realistic model representation of phytoplankton assemblages as well as their responses to multiple drivers. Future studies are needed to elucidate further multifactorial environmental changes, addressing both abiotic (e.g. changes in light and nutrients) as well as biotic (e.g. heterotrophy, competition, grazers, viruses) interactions.

Author Contributions

C.J.M.H. and B.R. designed the study. C.J.M.H. and C.F. conducted the experiment. C.J.M.H.

analysed the data and prepared the manuscript with contributions from B.R. and C.F.

The authors declare that they have no conflict of interest.

Acknowledgements

We are grateful for field support by the 2014/15 station team of the AWIPEV base in Ny-

Ålesund (Svalbard) as well as K. Wolf's help with strain isolation and maintenance of *M.*

pusilla cultures. We thank U. John and N. Kühne for sequencing and help with the molecular

strain identification. Furthermore, L. Wischnewski, A. Terbrüggen and M. Machnik are

acknowledged for their help with sample analyses.

References

AMAP: AMAP Assessment 2013: Arctic Ocean Acidification, Arctic Monitoring and Assessment Programme (AMAP), Oslo, Norway, 99, 2013.

Arrigo, K. R., van Dijken, G., and Pabi, S.: Impact of a shrinking Arctic ice cover on marine primary production, Geophysical Research Letters, 35, L19603, 10.1029/2008gl035028, 2008.

Bach, L. T., Mackinder, L. C. M., Schulz, K. G., Wheeler, G., Schroeder, D. C., Brownlee, C., and Riebesell, U.: Dissecting the impact of CO_2 and pH on the mechanisms of photosynthesis and calcification in the coccolithophore Emiliania huxleyi, New Phytologist, n/a-n/a, 10.1111/nph.12225, 2013.

Behrenfeld, M. J., Halsey, K. H., and Milligan, A. J.: Evolved physiological responses of phytoplankton to their integrated growth environment, Philosophical Transactions of the Royal Society B: Biological Sciences, 363, 2687-2703, 10.1098/rstb.2008.0019, 2008.

Berge, J., Daase, M., Renaud, Paul E., Ambrose, William G., Jr., Darnis, G., Last, Kim S., Leu, E., Cohen, Jonathan H., Johnsen, G., Moline, Mark A., Cottier, F., Varpe, Ø., Shunatova, N., Bałazy, P., Morata, N., Massabuau, J.-C., Falk-Petersen, S., Kosobokova, K., Hoppe, Clara J. M., Węsławski, Jan M., Kukliński, P., Legeżyńska, J., Nikishina, D., Cusa, M., Kędra, M., Włodarska-Kowalczuk, M., Vogedes, D., Camus, L., Tran, D., Michaud, E., Gabrielsen, Tove M., Granovitch, A., Gonchar, A., Krapp, R., and Callesen, Trine A.: Unexpected Levels of Biological Activity during the Polar Night Offer New Perspectives on a Warming Arctic, Curr. Biol., 25, 2555-2561, 10.1016/j.cub.2015.08.024, 2015.

Brewer, P. G., Bradshaw, A. L., and Williams, R. T.: Measurement of total carbon dioxide and alkalinity in the North Atlantic ocean in 1981, in: The Changing Carbon Cycle – A Global Analysis edited by: Trabalka, J. R., and Reichle, D. E., Springer Verlag, Heidelberg Berlin, 358–381, 1986.

Brown, J. H., Gillooly, J. F., Allen, A. P., Savage, V. M., and West, G. B.: Toward a metabolic theorie of ecology, Ecology, 85, 1771-1789, 10.1890/03-9000, 2004.

Brussaard, C. P. D., Noordeloos, A. A. M., Witte, H., Collenteur, M. C. J., Schulz, K., Ludwig, A., and Riebesell, U.: Arctic microbial community dynamics influenced by elevated CO_2 levels, Biogeosciences, 10, 719-731, 10.5194/bg-10-719-2013, 2013.

Collins, M., Knutti, R., Arblaster, J., Dufresne, J.-L., Fichefet, T., Friedlingstein, P., Gao, X., Gutowski, W., Johns, T., and Krinner, G.: Long-term climate change: projections, commitments and irreversibility, 2013.

Collins, S., Rost, B., and Rynearson, T. A.: Evolutionary potential of marine phytoplankton under ocean acidification, Evolutionary Applications, 7, 140-155, 10.1111/eva.12120, 2014.

Daufresne, M., Lengfellner, K., and Sommer, U.: Global warming benefits the small in aquatic ecosystems, Proceedings of the National Academy of Sciences, 106, 12788-12793, 10.1073/pnas.0902080106, 2009.

Dickson, A. G., and Millero, F. J.: A comparison of the equilibrium constants for the dissociation of carbonic acid in seawater media, Deep-Sea Research, 34, 1733– 1743, 1987.

Dickson, A. G.: Standard potential of the reaction: $AgCl(s) + ½ H_2(g) = Ag(s) + HCl(aq)$, and the standard acidity constant of the ion HSO_4^- in synthetic seawater from 273.15 to 318.15 K, Journal of Chemical Thermodynamics, 22, 113-127, 10.1016/0021-9614(90)90074-Z, 1990.

Dickson, A. G., Sabine, C. L., and Christian, J. R.: Guide to best practices for ocean CO_2 measurements, North Pacific Marine Science Organization, Sidney, British Columbia, 191, 2007.

Engel, A., Schulz, K. G., Riebesell, U., Bellerby, R., Delille, B., and Schartau, M.: Effects of CO_2 on particle size distribution and phytoplankton abundance during a mesocosm bloom experiment (PeECE II), Biogeosciences, 5, 509-521, 10.5194/bg-5-509-2008, 2008.

Eppley, R. W.: Temperature and phytoplankton growth in the sea, Fish. Bull, 70, 1063-1085, 1972.

Flynn, K. J., Blackford, J. C., Baird, M. E., Raven, J. A., Clark, D. R., Beardall, J., Brownlee, C., Fabian, H., and Wheeler, G. L.: Changes in pH at the exterior surface of plankton with ocean acidification, Nature Clim. Change, 2, 510-513, 2012.

Genty, B., Briantais, J.-M., and Baker, N. R.: The relationship between the quantum yield of photosynthetic electron transport and quenching of chlorophyll fluorescence, Biochimica et Biophysica Acta (BBA) - General Subjects, 990, 87-92, 10.1016/s0304-4165(89)80016-9, 1989.

Guillard, R. R. L., and Ryther, J. H.: Studies of marine planktonic diatoms. I. Cyclothella nana Hustedt and Detonula confervacea Cleve Can. J. Microbiol., 8, 229-239, 1962.

Halsey, K., Milligan, A., and Behrenfeld, M.: Contrasting Strategies of Photosynthetic Energy Utilization Drive Lifestyle Strategies in Ecologically Important Picoeukaryotes, Metabolites, 4, 260-280, 2014.

Halsey, K. H., and Jones, B. M.: Phytoplankton Strategies for Photosynthetic Energy Allocation, Annual Review of Marine Science, 7, 265-297, doi:10.1146/annurev-marine-010814-015813, 2015.

Harley, C. D. G., Connell, S. D., Doubleday, Z. A., Kelaher, B., Russell, B. D., Sarà, G., and Helmuth, B.: Conceptualizing ecosystem tipping points within a physiological framework, Ecology and Evolution, 10.1002/ece3.3164, 2017.

Hegseth, E. N., Assmy, P., Wiktor, J., Kristiansen, S., Leu, E., Tverberg, V., Gabrielsen, G. W., Skogseth, R., and Cottier, F. R.: Phytoplankton seasonal dynamics in Kongsfjorden,

Svalbard and the adjacent shelf, in: The Ecosystem of Kongsfjorden, Svalbard, edited by: Hop, H., and Wiencke, C., Springer, in press.

Hoppe, C. J. M., Langer, G., Rokitta, S. D., Wolf-Gladrow, D. A., and Rost, B.: Implications of observed inconsistencies in carbonate chemistry measurements for ocean acidification studies, Biogeosciences, 9, 2401–2405, 10.5194/bg-9-2401-2012, 2012.

Hoppe, C. J. M., Holtz, L.-M., Trimborn, S., and Rost, B.: Ocean acidification decreases the light-use efficiency in an Antarctic diatom under dynamic but not constant light, New Phytologist, 207, 159-171, 10.1111/nph.13334, 2015.

Hussherr, R., Levasseur, M., Lizotte, M., Tremblay, J. É., Mol, J., Thomas, H., Gosselin, M., Starr, M., Miller, L. A., Jarniková, T., Schuback, N., and Mucci, A.: Impact of ocean acidification on Arctic phytoplankton blooms and dimethyl sulfide concentration under simulated ice-free and under-ice conditions, Biogeosciences, 14, 2407-2427, 10.5194/bg-14-2407-2017, 2017.

Knap, A., Michaels, A., Close, A., Ducklow, H., and Dickson, A..: Protocols for the Joint Global Ocean Flux Study (JGOFS) Core Measurements., UNESCO, 170, 1996.

Kolber, Z. S., Prasil, O., and Falkowski, P. G.: Measurements of variable chlorophyll fluorescence using fast repetition rate techniques. I. Defining methodology and experimental protocols, Biochem. Biophys. Acta, 1367, 88-106, 1998.

Kranz, S. A., Young, J. N., Hopkinson, B. M., Goldman, J. A. L., Tortell, P. D., and Morel, F. M. M.: Low temperature reduces the energetic requirement for the CO_2 concentrating mechanism in diatoms, New Phytologist, 205, 192-201, 10.1111/nph.12976, 2015.

Levitt, J.: Responses of Plants to Environmental Stress, Volume 1: Chilling, Freezing, and High Temperature Stresses, Academic Press., 1980.

Li, W. K. W., McLaughlin, F. A., Lovejoy, C., and Carmack, E. C.: Smallest Algae Thrive As the Arctic Ocean Freshens, Science, 326, 539, 10.1126/science.1179798, 2009.

Lovejoy, C., Vincent, W. F., Bonilla, S., Roy, S., Martineau, M.-J., Terrado, R., Potvin, M., Massana, R., and Pedrós-Alió, C.: Distribution, phylogeny, and growth of cold-adapted picoprasinophytes in Arctic Seas, Journal of Phycology, 43, 78-89, 10.1111/j.1529-8817.2006.00310.x, 2007.

Lovejoy, C.: Changing Views of Arctic Protists (Marine Microbial Eukaryotes) in a Changing Arctic, Acta Protozool., 53, 91-100, 10.4467/16890027ap.14.009.1446, 2014.

Maat, D. S., Crawfurd, K. J., Timmermans, K. R., and Brussaard, C. P. D.: Elevated CO_2 and Phosphate Limitation Favor Micromonas pusilla through Stimulated Growth and Reduced Viral Impact, Applied and Environmental Microbiology, 80, 3119-3127, 10.1128/aem.03639-13, 2014.

Marquardt, M., Vader, A., Stübner, E. I., Reigstad, M., and Gabrielsen, T. M.: Strong Seasonality of Marine Microbial Eukaryotes in a High-Arctic Fjord (Isfjorden, in West Spitsbergen, Norway), Applied and Environmental Microbiology, 82, 1868-1880, 10.1128/aem.03208-15, 2016.

Maxwell, D. P., Falk, S., Trick, C. G., and Huner, N.: Growth at Low Temperature Mimics High-Light Acclimation in Chlorella vulgaris, Plant Physiology, 105, 535-543, 10.1104/pp.105.2.535, 1994.

Maxwell, K., and Johnson, G. N.: Chlorophyll fluorescence a practical guide, J. Exp. Bot., 51, 659-668, 10.1093/jexbot/51.345.659, 2000.

McKew, B. A., Davey, P., Finch, S. J., Hopkins, J., Lefebvre, S. C., Metodiev, M. V., Oxborough, K., Raines, C. A., Lawson, T., and Geider, R. J.: The trade-off between the light-harvesting and photoprotective functions of fucoxanthin-chlorophyll proteins dominates light acclimation in *Emiliania huxleyi* (clone CCMP 1516), New Phytologist, 200, 74-85, 10.1111/nph.12373, 2013.

McKie-Krisberg, Z. M., and Sanders, R. W.: Phagotrophy by the picoeukaryotic green alga *Micromonas*: implications for Arctic Oceans, ISME J, 8, 1953-1961, 10.1038/ismej.2014.16, 2014.

Meakin, N. G., and Wyman, M.: Rapid shifts in picoeukaryote community structure in response to ocean acidification, ISME J, 5, 1397-1405, 2011.

Mehrbach, C., Culberson, C. H., Hawley, J. E., and Pytkowicz, R. M.: Measurement of the apparent dissociation constants of carbonic acid in seawater at atmospheric pressure, Limnology and Oceanography, 18, 897–907, 10.4319/lo.1973.18.6.0897, 1973.

Miller, G. H., Alley, R. B., Brigham-Grette, J., Fitzpatrick, J. J., Polyak, L., Serreze, M. C., and White, J. W. C.: Arctic amplification: can the past constrain the future?, Quaternary Science Reviews, 29, 1779-1790, 10.1016/j.quascirev.2010.02.008, 2010.

Mock, T., and Hoch, N.: Long-Term Temperature Acclimation of Photosynthesis in Steady-State Cultures of the Polar Diatom *Fragilariopsis cylindrus*, Photosynth Res, 85, 307-317, 10.1007/s11120-005-5668-9, 2005.

Morgan-Kiss, R. M., Priscu, J. C., Pocock, T., Gudynaite-Savitch, L., and Huner, N. P. A.: Adaptation and Acclimation of Photosynthetic Microorganisms to Permanently Cold Environments, Microbiology and Molecular Biology Reviews, 70, 222-252, 10.1128/mmbr.70.1.222-252.2006, 2006.

Newbold, L. K., Oliver, A. E., Booth, T., Tiwari, B., DeSantis, T., Maguire, M., Andersen, G., van der Gast, C. J., and Whiteley, A. S.: The response of marine picoplankton to ocean acidification, Environmental Microbiology, 14, 2293-2307, 10.1111/j.1462-2920.2012.02762.x, 2012.

Oxborough, K.: FastPro8 GUI and FRRf3 systems documentation. Chelsea Technologies Group Ltd 2012, 2012.

Paulsen, M. L., Riisgaard, K., Frede, T., St John, M., and Nielsen, T. G.: Winter− spring transition in the subarcticAtlantic: microbial response to deep mixingand pre-bloom production, 2015.

Pierrot, D. E., Lewis, E., and Wallace, D. W. R.: MS Exel Program Developed for CO2 System Calculations. ORNL/CDIAC-105aCarbon Dioxide Information Analysis Centre, O. R. N. L. (Ed.), US Department of Energy, Oak Ridge, Tennessee, 2006.

Post, E.: Implications of earlier sea ice melt for phenological cascades in arctic marine food webs, Food Webs, 10.1016/j.fooweb.2016.11.002, 2016.

Qi, D., Chen, L., Chen, B., Gao, Z., Zhong, W., Feely, R. A., Anderson, L. G., Sun, H., Chen, J., Chen, M., Zhan, L., Zhang, Y., and Cai, W.-J.: Increase in acidifying water in the western Arctic Ocean, Nature Clim. Change, 7, 195-199, 10.1038/nclimate3228, 2017.

Raven, J.: The twelfth Tansley Lecture. Small is beautiful: the picophytoplankton, Funct. Ecol., 12, 503-513, 1998.

Richardson, T. L., and Jackson, G. A.: Small Phytoplankton and Carbon Export from the Surface Ocean, Science, 315, 838-840, 10.1126/science.1133471, 2007.

Riebesell, U., and Gattuso, J.-P.: Lessons learned from ocean acidification research, Nature Climate Change, 5, 12-14, 2015.

Rost, B., Zondervan, I., and Wolf-Gladrow, D.: Sensitivity of phytoplankton to future changes in ocean carbonate chemistry: Current knowledge, contradictions and research needs, Mar. Ecol. Prog. Ser., 373, 227-237, 10.3354/meps07776, 2008.

Sarthou, G., Timmermans, K. R., Blain, S., and Tréguer, P.: Growth physiology and fate of diatoms in the ocean: a review, J. Sea Res., 53, 25-42, 10.1016/j.seares.2004.01.007, 2005.

Schaum, E., Rost, B., Millar, A. J., and Collins, S.: Variation in plastic responses of a globally distributed picoplankton species to ocean acidification, Nature Climate Change, 3, 298–302, 10.1038/nclimate1774, 2012.

Schulz, K. G., Bellerby, R. G. J., Brussaard, C. P. D., Büdenbender, J., Czerny, J., Engel, A., Fischer, M., Koch-Klavsen, S., Krug, S. A., Lischka, S., Ludwig, A., Meyerhöfer, M., Nondal, G., Silyakova, A., Stuhr, A., and Riebesell, U.: Temporal biomass dynamics of an Arctic plankton bloom in response to increasing levels of atmospheric carbon dioxide, Biogeosciences, 10, 161 - 180, 10.5194/bg-10-161-2013, 2013.

Schulz, K. G., Bach, L. T., Bellerby, R. G. J., Bermúdez, R., Büdenbender, J., Boxhammer, T., Czerny, J., Engel, A., Ludwig, A., Meyerhöfer, M., Larsen, A., Paul, A. J., Sswat, M., and Riebesell, U.: Phytoplankton Blooms at Increasing Levels of Atmospheric Carbon Dioxide:

Experimental Evidence for Negative Effects on Prymnesiophytes and Positive on Small Picoeukaryotes, Frontiers in Marine Science, 4, 10.3389/fmars.2017.00064, 2017.

Sett, S., Schulz, K. G., Bach, L. T., and Riebesell, U.: Shift towards larger diatoms in a natural phytoplankton assemblage under combined high-CO_2 and warming conditions, J. Plankton Res., 10.1093/plankt/fby018, 2018.

Sett, S., Bach, L. T., Schulz, K. G., Koch-Klavsen, S., Lebrato, M., and Riebesell, U.: Temperature Modulates Coccolithophorid Sensitivity of Growth, Photosynthesis and Calcification to Increasing Seawater pCO_2, PLoS ONE, 9, e88308, 10.1371/journal.pone.0088308, 2014.

Sherr, E. B., and Sherr, B. F.: Significance of predation by protists in aquatic microbial food webs, Antonie Leeuwenhoek, 81, 293-308, 10.1023/a:1020591307260, 2002.

Sherr, E. B., Sherr, B. F., Wheeler, P. A., and Thompson, K.: Temporal and spatial variation in stocks of autotrophic and heterotrophic microbes in the upper water column of the central Arctic Ocean, Deep Sea Research Part I: Oceanographic Research Papers, 50, 557-571, 10.1016/S0967-0637(03)00031-1, 2003.

Silsbe, G. M., and Kromkamp, J. C.: Modeling the irradiance dependency of the quantum efficiency of photosynthesis, Limnol. Oceanogr. Methods, 10, 645-652, 2012.

Šlapeta, J., López-García, P. n., and Moreira, D.: Global Dispersal and Ancient Cryptic Species in the Smallest Marine Eukaryotes, Mol. Biol. Evol., 23, 23-29, 10.1093/molbev/msj001, 2006.

Sommer, U., Paul, C., and Moustaka-Gouni, M.: Warming and ocean acidification effects on phytoplankton—from species shifts to size shifts within species in a mesocosm experiment, PLoS One, 10, e0125239, 2015.

Stocker, T.: Climate change 2013: the physical science basis: Working Group I contribution to the Fifth assessment report of the Intergovernmental Panel on Climate Change, Cambridge University Press, 2014.

Stoll, M. H. C., Bakker, K., Nobbe, G. H., and Haese, R. R.: Continous-Flow Analysis of Dissolved Inorganic Carbon Content in Seawater, Analytical Chemistry, 73, 4111-4116, 2001.

Suggett, D. J., Borowitzka, M. A., and Prášil, O. E.: Chlorophyll a Fluorescence in Aquatic Sciences: Methods and Applications, Developments in Applied Phycology, Springer, Dordrecht, 326 pp., 2010.

Taylor, A. R., Chrachri, A., Wheeler, G., Goddard, H., and Brownlee, C.: A Voltage-Gated H^+ Channel Underlying pH Homeostasis in Calcifying Coccolithophores, PLoS Biol., 9, 10.1371/journal.pbio.1001085, 2001.

Toseland, A., Daines, S. J., Clark, J. R., Kirkham, A., Strauss, J., Uhlig, C., Lenton, T. M., Valentin, K., Pearson, G. A., Moulton, V., and Mock, T.: The impact of temperature on marine phytoplankton resource allocation and metabolism, Nature Clim. Change, 3, 979-984, 10.1038/nclimate1989, 2013.

Tremblay, G., Belzile, C., Gosselin, M., Poulin, M., Roy, S., and Tremblay, J. E.: Late summer phytoplankton distribution along a 3500 km transect in Canadian Arctic waters: strong numerical dominance by picoeukaryotes, Aquat. Microb. Ecol., 54, 55-70, 2009.

Tremblay, J.-É., Anderson, L. G., Matrai, P., Coupel, P., Bélanger, S., Michel, C., and Reigstad, M.: Global and regional drivers of nutrient supply, primary production and CO_2 drawdown in the changing Arctic Ocean, Progress in Oceanography, 139, 171-196, 10.1016/j.pocean.2015.08.009, 2015.

Vader, A., Marquardt, M., Meshram, A. R., and Gabrielsen, T. M.: Key Arctic phototrophs are widespread in the polar night, Polar Biol, 38, 13-21, 10.1007/s00300-014-1570-2, 2015.

van de Waal, D., and Boersma, M.: Ecological stoichiometry in aquatic ecosystems, in: Encyclopedia of Life Support Systems (EOLSS), Developed under the Auspices of the UNESCO (eds. UNESCO-EOLSS Joint Committee), Eolss Publishers, 2012.

Waite, A. M., Safi, K. A., Hall, J. A., and Nodder, S. D.: Mass sedimentation of picoplankton embedded in organic aggregates, Limnology and Oceanography, 45, 87-97, 10.4319/lo.2000.45.1.0087, 2000.

Wassmann, P., and Reigstad, M.: Future Arctic Ocean seasonal ice zones and implications for pelagic-benthic coupling, Oceanography, 24, 220-231, 10.5670/oceanog.2011.74., 2011.

Webb, W., Newton, M., and Starr, D.: Carbon dioxide exchange of *Alnus rubra*, Oecologia, 17, 281-291, 10.1007/bf00345747, 1974.

Wolf, K., Hoppe, C. J. M., and Rost, B.: Resilience by diversity: Large intraspecific differences in climate change responses of an Arctic diatom, Limnology and Oceanography, 63, 397-411, 10.1002/lno.10639, 2018.

Worden, A. Z., and Not, F.: Ecology and diversity of picoeukaryotes, Microbial Ecology of the Oceans, Second Edition, 159-205, 2008.

Worden, A. Z., Follows, M. J., Giovannoni, S. J., Wilken, S., Zimmerman, A. E., and Keeling, P. J.: Rethinking the marine carbon cycle: Factoring in the multifarious lifestyles of microbes, Science, 347, 10.1126/science.1257594, 2015.

Wu, Y., Campbell, D. A., Irwin, A. J., Suggett, D. J., and Finkel, Z. V.: Ocean acidification enhances the growth rate of larger diatoms, Limnology and Oceanography, 59, 1027-1034, 10.4319/lo.2014.59.3.1027, 2014.

Young, J. N., Goldman, J. A. L., Kranz, S. A., Tortell, P. D., and Morel, F. M. M.: Slow carboxylation of Rubisco constrains the rate of carbon fixation during Antarctic phytoplankton blooms, New Phytologist, 205, 172–181, 10.1111/nph.13021, 2014.

Zeebe, R. E., and Wolf-Gladrow, D. A.: CO_2 in Seawater: Equilibrium, Kinetics, Isotopes, Elsevier Science, Amsterdam, 2001.

Table 1: Seawater carbonate chemistry at the end of the experiments (n=3; mean ±1 s.d.). CO_2 partial pressure (pCO_2) and dissolved CO_2 concentrations were calculated from total alkalinity (A_T) and pH_{total} at 2 or 6°C, a salinity of 32.7 using CO_2SYS (Pierrot et al., 2006), and phosphate and silicate concentrations of 10 and 100 µmol kg^{-1}, respectively. n.a. indicates that values are not available for this specific treatment.

Temperature [°C]	pCO_2 level [µatm]	pH total scale	A_T [µmol kg^{-1}]	C_T [µmol kg^{-1}]	dissolved CO_2 [µmol kg^{-1}]	pCO_2 [µatm]
2	180	8.3 ± 0.01	2264 ± 9	2024 ± 6	11.6 ± 0.2	197 ± 3
	380	8.11 ± 0.01	2244 ± 30	2124 ± 11	19.0 ± 0.7	323 ± 12
	1000	7.68 ± 0.01	2255 ± 45	2215 ± 23	56.4 ± 1.3	959 ± 22
	1400	7.52 ± 0.02	2243 ± 5	n.a.	81.1 ± 3.1	1380 ± 53
6	180	8.3 ± 0.01	2243 ± 28	1969 ± 10	10.0 ± 0.3	198 ± 6
	380	8.04 ± 0.01	2256 ± 21	2058 ± 7	20.0 ± 0.5	394 ± 10
	1000	7.65 ± 0.01	2262 ± 22	2178 ± 14	52.6 ± 1.6	1036 ± 31
	1400	7.52 ± 0.01	2265 ± 5	n.a.	73.6 ± 0.9	1449 ± 18

Table 2: Growth rate constants μ, division rate constants k, POC production rates and cellular quota of Chl a, POC and PON as well as their ratios of *M. pusilla* at the end of the experiment under the different treatment conditions (n=3; mean ±1 s.d.). Results from statistical analysis can be found in Table SI2.

Temperature [°C]	pCO$_2$ [µatm]	Growth rate constant μ [d^{-1}]	Division rate constant k [d^{-1}]	POC production [fmol cell^{-1} d^{-1}]	POC quota [fmol cell^{-1}]	PON quota [fmol cell^{-1}]	Chl a quota [fg cell^{-1}]	POC:PON [mol mol^{-1}]	POC:Chl a [g g^{-1}]
2	180	0.75 ± 0.04	1.08 ± 0.05	256 ± 11	239 ± 20	28.7 ± 2.6	28.6 ± 2.1	8.3 ± 0.1	100 ± 7
	380	0.85 ± 0.03	1.23 ± 0.04	290 ± 16	237 ± 22	30.9 ± 1.8	24.7 ± 1.4	7.7 ± 0.3	115 ± 10
	1000	0.79 ± 0.05	1.15 ± 0.07	224 ± 23	196 ± 25	24.9 ± 4.9	20.0 ± 2.9	8.0 ± 0.6	118 ± 5
	1400	0.82 ± 0.05	1.18 ± 0.07	235 ± 13	199 ± 16	23.9 ± 2.3	22.0 ± 1.5	8.4 ± 0.1	109 ± 4
6	180	1.06 ± 0.03	1.53 ± 0.05	376 ± 15	245 ± 3	26.9 ± 0.6	21.1 ± 0.8	9.1 ± 0.1	140 ± 7
	380	1.05 ± 0.03	1.52 ± 0.04	342 ± 39	226 ± 26	25.9 ± 2.5	22.1 ± 2.6	8.7 ± 0.3	123 ± 11
	1000	1.25 ± 0.05	1.80 ± 0.07	497 ± 12	275 ± 6	33.7 ± 2.0	27.2 ± 0.9	8.2 ± 0.6	122 ± 6
	1400	1.05 ± 0.04	1.52 ± 0.06	400 ± 14	263 ± 7	31.1 ± 1.7	28.6 ± 3.2	8.5 ± 0.3	111 ± 16

Table 3: **:** FRR-flourometrical PSII photochemistry measurements – PSII quantum yield efficiency Fv/Fm [dimensionless], functional absorption cross section (σ_{PSII}) [nm^{-2} PSII^{-1}]), rate of PSII re-opening (τ_{ES} [ms]), maximum non-photochemical quenching at 672 µmol photons m^{-2} s^{-1} (NPQ$_{max}$ [dimensionless]), maximum light-use efficiency (initial slope α [mol e^{-} m^2 (mol RCII)$^{-1}$ (mol photons)$^{-1}$]), maximal absolute electron transfer rates through PSII (ETR$_{max}$ [mol e^{-} (mol RCII)$^{-1}$ s^{-1}]), and the light saturation index (E$_K$ [µmol photons m^{-2} s^{-1}]) under the different temperature and pCO$_2$ treatments (n=3; mean ±1 s.d.). Results from statistical analysis can be found in Table SI2.

Temp	pCO$_2$	Fv/Fm	σ_{PSII}	τ_{ES}	NPQ$_{max}$	α	ETR$_{max}$	E$_K$
2	180	0.50 ± 0.01	8.66 ± 0.35	439 ± 8	2.26 ± 0.18	0.42 ± 0.05	33 ± 2	81 ± 13
	380	0.43 ± 0.09	8.93 ± 0.26	425 ± 4	3.51 ± 0.55	0.32 ± 0.15	25 ± 5	91 ± 44
	1000	0.45 ± 0.08	8.55 ± 0.07	448 ± 1	3.96 ± 0.71	0.42 ± 0.03	31 ± 2	75 ± 10
	1400	0.47 ± 0.10	9.06 ± 0.05	422 ± 14	2.45 ± 0.44	0.43 ± 0.08	31 ± 7	75 ± 31
6	180	0.49 ± 0.01	9.22 ± 0.22	412 ± 6	2.51 ± 0.37	0.49 ± 0.08	28 ± 10	59 ± 28
	380	0.43 ± 0.12	8.83 ± 0.17	427 ± 6	2.83 ± 0.59	0.38 ± 0.09	35 ± 14	90 ± 17
	1000	0.41 ± 0.07	8.91 ± 0.22	422 ± 11	4.94 ± 1.46	0.33 ± 0.09	32 ± 5	100 ± 21
	1400	0.45 ± 0.04	8.71 ± 0.50	428 ± 19	2.93 ± 0.50	0.38 ± 0.04	40 ± 5	104 ± 6

Figure 1: Specific growth rate constant μ (A) and POC production (B) of *M. pusilla* under low (filled symbols) and high temperatures (open symbols) as a function of pCO_2 (n=3; mean ±1 s.d.). Results from statistical analysis can be found in Table SI2.
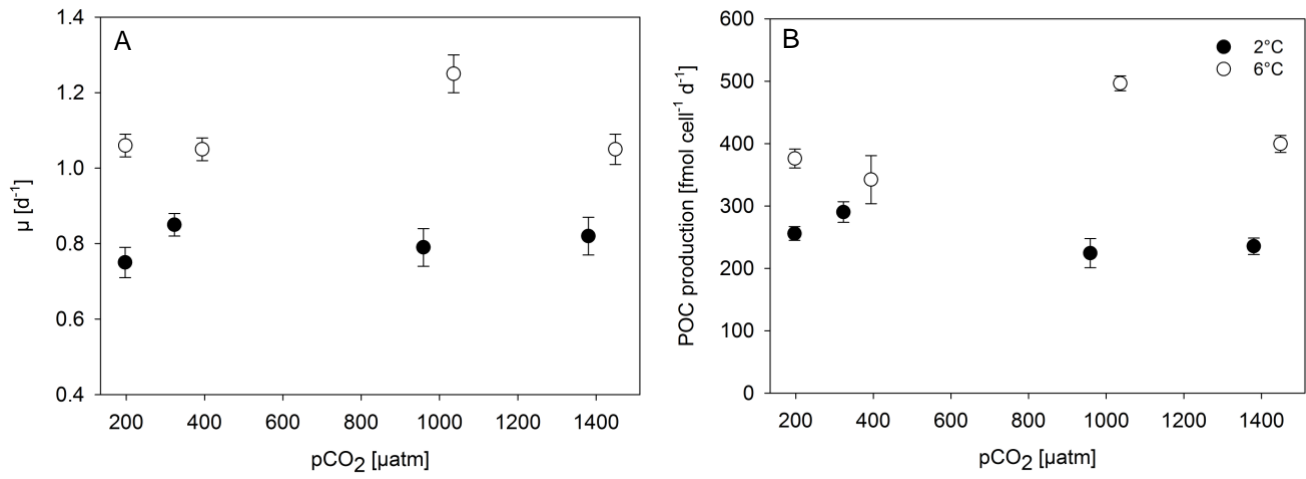
Figure 2: Cellular composition, i.e. POC (A), PON (B) and Chl *a* quota (C) as well as as C:Chl *a* ratios (D), of *M. pusilla* under low (filled symbols) and high temperatures (open symbols) as a function of pCO$_2$ (n=3; mean ±1 s.d.). Results from statistical analysis can be found in Table SI2.
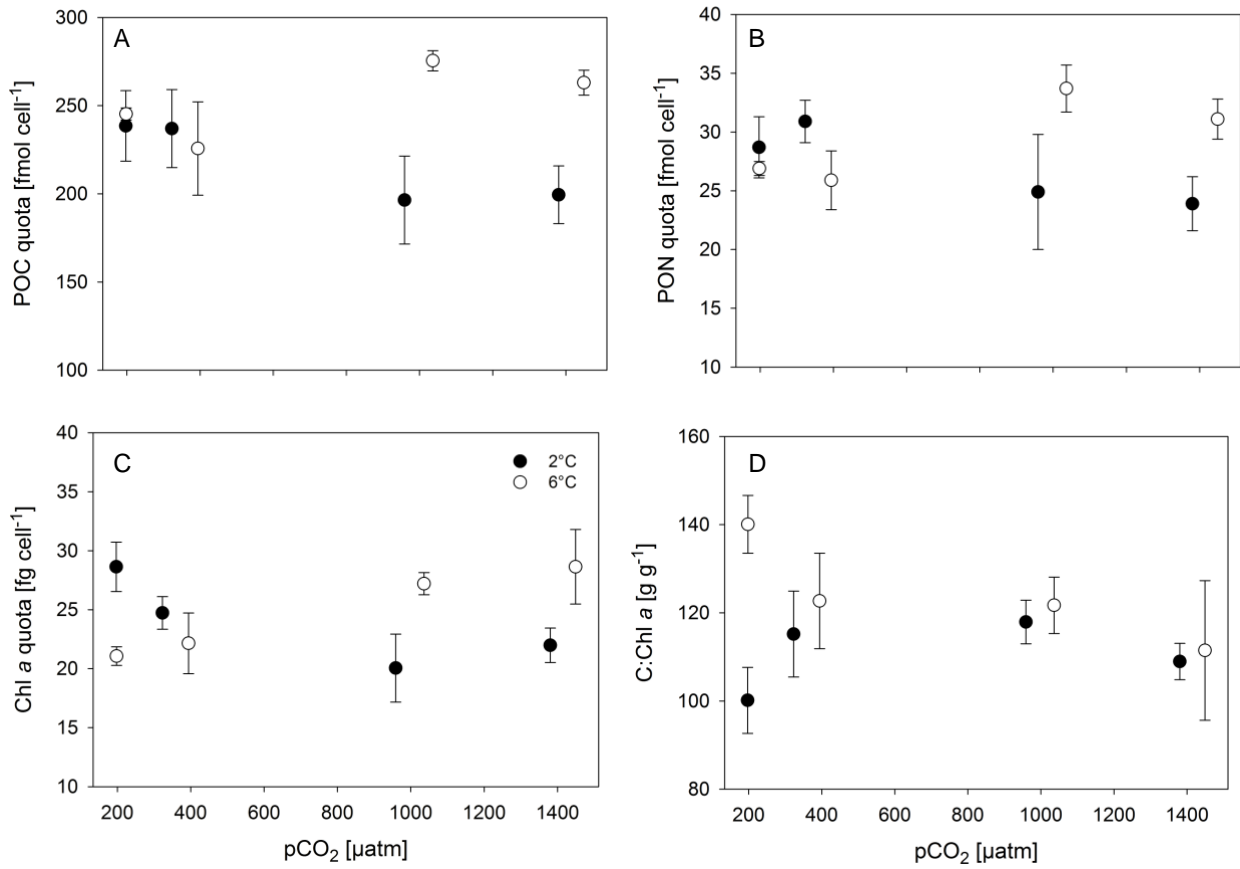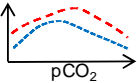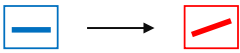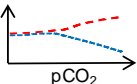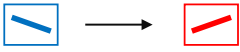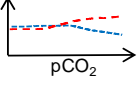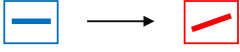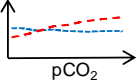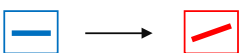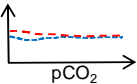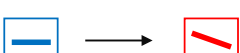
Figure 3: Schematic illustration of results for both temperatures over the entire range of pCO_2 levels as well as focusing on the responses between 380 and 1000 µatm (as the representation for commonly used OA treatments) and their modulation by temperature.